Iranian Journal of Catalysis 6(3), 2016, 221-228

IRANIAN JOURNAL OF CATALYSIS

Synthesis and photocatalytic activity of nanosized modified mesocellulous silica foams (MCFs) with PW_{12} and vanadium oxide

Leili Shabani, Hamid Aliyan*

Department of Chemistry, Shahreza Branch, Islamic Azad University, 86145-311, Iran.

Received 9 December 2014; received in revised form 24 July 2015; accepted 26 September 2015

ABSTRACT

A series of tungestophosphoric acid and vanadium oxide supported on Mesocellulous Silica Foams (MCFs) featuring a well-defined three-dimensional (3D) mesoporosity were studied with regard to their performance in the photocatalytic activity to degrade Oezine Y (OY). This nanosized mesoporous catalyst (PW_{12}@V-MCF) was characterized by FTIR, XRD, BET and TEM. XRD shows that the structure of MCF remains intact after PW_{12} modification, while spectral techniques show the successful grafting of the PW_{12} on the MCF cavities. PW_{12}-MCF was used as a catalyst in the photodecolorization process of Oezine Y (OY) dye in aqueous solution under UV radiation. It was found that the catalyst exhibited significantly high catalytic stability, and the activity loss is negligible after three OY degradation cycles.

***Keywords**: Mesocellular silica foam (MCF), Impregnation, Heterogeneous photocatalysis, Polyoxotungstate.*

1. Introduction

Dye pollutants from the textile industry are important sources of environmental contamination. It is estimated that from 1 to 15% of dye is lost during dyeing processes and is released in waste waters [1]. The release of these colored waste waters in the eco system is a dramatic source of aesthetic pollution, eutrophication and perturbations in aquatic life [2]. A variety of physical, chemical and biological methods are presently available for the treatment of textile waste water. Biological treatment is a proven technology and is cost effective. However, it has been reported that the majority of dyes are only adsorbed into the sludge and are not degraded [3]. Physical methods such as ion exchange, adsorption, air stripping, etc., are also ineffective on pollutants which are not readily adsorbable or volatile, and have the further disadvantage that they simply transfer the pollutants to another phase rather than destroying them. This leads to search for a highly effective method to degrade the dyes into environmentally compatible products [4-14].

*Corresponding author email: aliyan@iaush.ac.ir
Tel.:+98 31 5350 2706-7; Fax: +98 31 5350 2701

Ordered mesoporous silicas represent a class of materials that can be used as adsorbents [15]. The most important characteristics of the mesoporous silicas are the large surface area, high mesopore volume, and narrow pore size distribution in the range of mesopores. However, many applications (such as adsorption, ion exchange, catalysis and sensing) require these silica-based materials to have specific attributes such as binding sites, stereochemical configuration, charge density and acidity [16]. Functionalization of the silica surface with organic groups is very important and can be achieved via post synthesis grafting or direct co-condensation synthesis routes [17,18].

The photochemical behaviour of polyoxometalates (POMs) has been studied extensively in homogeneous systems, and it indicates that the photo-oxidation efficiency of POMs is comparable to that of the semiconductor TiO_2 [19-26]. The major drawback to the practical applications of POM photocatalytic systems is the high water solubility of POMs, which impedes ready recovery and reuse of the photocatalysts [27]. Otherwise, the active sites on the surface of the catalyst are small because of the low specific surface areas of solid POMs (ca. $5 m^2/g$). Therefore, two main methods for the preparation of insoluble POMs are

considered, i.e. precipitation with a counter-cation such as Cs+ to form $Cs_3PW_{12}O_{40}$ colloidal [28], and immobilization of POMs into the solid matrix [29]. The latter is much more interesting because the support makes POMs easily handled and recycled [30-33].

In this study, we report on the catalytic behaviour of MCF-supported vanadium and $H_3PW_{12}O_{40}$ (donated by PW_{12}, hereafter) photocatalysts for degradation of Oezine Y (OY) (Scheme 1).

The influences of experimental parameters were studied to achieve a better degradation efficiency of dyes. Choosing OY dye as a pollutant molecule is because of its importance as dye in textile industry and other various applications [34-36]. The colour removal of dye solutions without catalyst was studied in all experiments. To our knowledge, this is first study of PW_{12} @V-MCF toward OY photodecolorizations.

2. Experimental

All materials were commercial reagent grade. Dye chemical structures are shown in Table 1. Infrared spectra (400–4000 cm^{-1}) were recorded from KBr pellets on a Nicolet *Impact 400 D* spectrometer. The X-ray powdered diffraction patterns were performed on a Bruker-D8 advance with automatic control. The patterns were run with monochromatic Cu Kα (1.5406 Å) radiation with a scan rate of 2º min^{-1}. Nitrogen adsorption measurements were performed at −196°C by using an ASAP 2010M surface analyser, and the pre-treatment temperature was 180 °C. Transmission electron micrographs (TEM) were obtained on a Joel JEM 2010 scan-transmission electron microscope. The sample for the TEM measurement was suspended in ethanol and supported on a carbon coated copper grid. The UV light source was an Hg lamp (75 W). The absorption spectra were registered on a double beam spectrophotometer (Carry 100 Scan) in suprasil quartz cells of 1 cm optical path length and the absorbance of samples was measured in the wavelength range of 190-900 nm. In order to remove photocatalyst particles before analysis, the suspensions were centrifuged with "type-H-11n" and 3500 rpm for 5 min. The influence of pH on the absorption was studied by adding HCl or NaOH solutions to the suspensions.

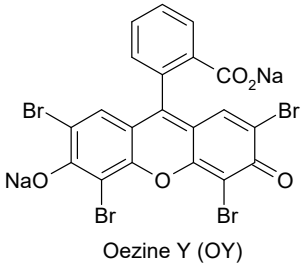

Oezine Y (OY)

Scheme 1. The structures of the used commercial dye.

2.1. Catalysts synthesis

2.1.1. MCF

The purely siliceous MCF sample was prepared as described previously [37] using a Pluronic P123 triblock copolymer ($EO_{20}PO_{70}EO_{20}$, *M*av = 5800, Aldrich) surfactant with 1,3,5-trimethylbenzene (TMB) as the organic swelling agent with TMB/P123 = 0.5 (w/w). In a typical preparation, a solution of P123: TMB:1.6 M HCl:TEOS = 2:1:75:4.25 (mass ratio) was prepared at room temperature, then heated to 40°C. After 24 h at 40°C, the milky reaction mixture was transferred to an autoclave and aged at 100°C for another 24 h. The solid products were filtered off and dried overnight at 100°C under static conditions. The surfactant was removed by calcinations at 600°C for 5 h in air, yielding the final mesoporous MCF material.

2.1.2. Preparation of V@MCF

MCF-supported vanadia catalysts were prepared by an alcoholic impregnation method as described previously [38]. A methanol solution of NH_4VO_3 to achieve a final V content of 1.4–5.6 wt% of V atoms was contacted with the MCF carrier at 60°C, and the methanol was rota evaporated until complete dryness. Then the catalysts were dried overnight in air at 120°C, followed by calcination at 600 °C for 4 h in air.

2.1.3. PW_{12}@V-MCF

PW_{12}@V-MCF was prepared by incipient wetness method: mixing 50 mg of PW_{12} and 100 mg of the V-MCF sample with 10 mL of distilled water in an Erlenmeyer flask at room temperature and under stirring for 12 h. The resulting pastes were dried for 4 h at 100ºC and calcined for 4 h at 400ºC (Scheme 2).

2.2. Photocatalytic activity

Photodegredation experiments were performed with a photocatalytic reactor system. The bench-scale system is a cylindrical Pyrex-glass cell with 1.0 L capacity, 10 cm inside diameter and 15 cm height. Irradiation experiments were performed using medium pressure Hg lamp (75 W), then it was placed in a 5 cm diameter quartz tube with one end tightly sealed by a Teflon stopper. The inner tube containing the lamp was placed directly into the outer Pyrex tube so that the solution was between the two tubes and directly exposed to the UV emanating from the quartz tube. The lamp and the tube were then immersed in the photoreactor cell with a light path of 3.0 cm. A magnetic stirrer was used continuously to guarantee good mixing of the solution. Generally, HCl (1M) and NaOH (1M) were used to

$$PW_{12} + \text{V-MCF} \xrightarrow[H_2O,\ r.t]{\text{assembly}} \xrightarrow[\text{for 4 h at 100 }^oC]{\text{were dried}} \xrightarrow[\text{for 4 h at 400 }^oC]{\text{were calcined}} PW_{12}@\text{V-MCF}_{IMPREGNATE}$$

Scheme 2. Preparation of HPA@V-MCF IMPREGNATED

adjust the pH value in the beginning of all experiments including the effect of pH study. The decolorization of the commercial dye OY was analyzed by UV-Vis spectrophotometer (Carry 100 Scan). In the investigation of pH, due to shift in the λ_{max} value, new λ_{max} was determined by scanning the samples in range of 190-900 nm. Decolorization efficiency was determined using absorbance of solutions before and after photodecolorization experiments. To determine the surface adsorption amount, control experiments in the dark condition were carried out in parallel in each case at the presence of catalyst on the decolorozation of the mentioned OY dye.

3. Results and Discussion

3.1 Physico-chemical characterization

3.1.1. FTIR

Fig. 1 presents the FTIR spectra in the skeletal region of 4000–400 cm^{-1} for the V-loaded MCF materials. As shown in the spectrum of the parent MCF silica, the typical bands due to siliceous Si–O–Si material are observed: A main band at 1070 cm^{-1} with a shoulder at 1200 cm^{-1}, due to asymmetric Si–O–Si stretching modes, the corresponding symmetric stretch at 810 cm^{-1}, and Si–O– or Si–OH at 972 cm^{-1} [39]. In the spectra of the V-containing samples, an additional band at ca. 915 cm^{-1}, indicative of Si–O–V species [40], is well developed for the samples with V content up to 5.6 wt%. Coupled with the significant spectral changes in the hydroxyl region, these phenomena further confirm the perturbed silica vibrations due to the incorporation of vanadium into the MCF silica framework. Other researchers have reported similar trends in the IR spectra of their catalytic vanadia-silicas [38-42].

FT-IR spectra have been proven to be a powerful technique for the study of surface interaction between heteropolyacid and organic and inorganic supports. The FTIR spectrum of 50 wt.% samples of PW_{12} @ V-MCF (Fig. 2) shows four bands in the range 1250–500 cm^{-1}. It was found that for 110oC dried samples the Keggin bands are observed at 1097, 960, 890 and 810 cm^{-1} for PW_{12}@MCF.

3.1.2. XRD

Fig. 3a shows the XRD patterns of pure MCF within the 2θ range of 5–70°. The peaks corresponding to amorphous MCF are present. Wide-angle XRD patterns of the V@MCF samples with various V content are shown in Fig. 3d-3e. No diffraction peaks corresponding to vanadium oxides were detected in the V@MCF catalysts with a V content of up to 5.6% suggest that the vanadium species in these samples are highly dispersed on the surface. As the V content was increased to 8%, weak diffraction peaks of crystalline V_2O_5 appeared indicating the formation of bulk vanadia at a high V content.

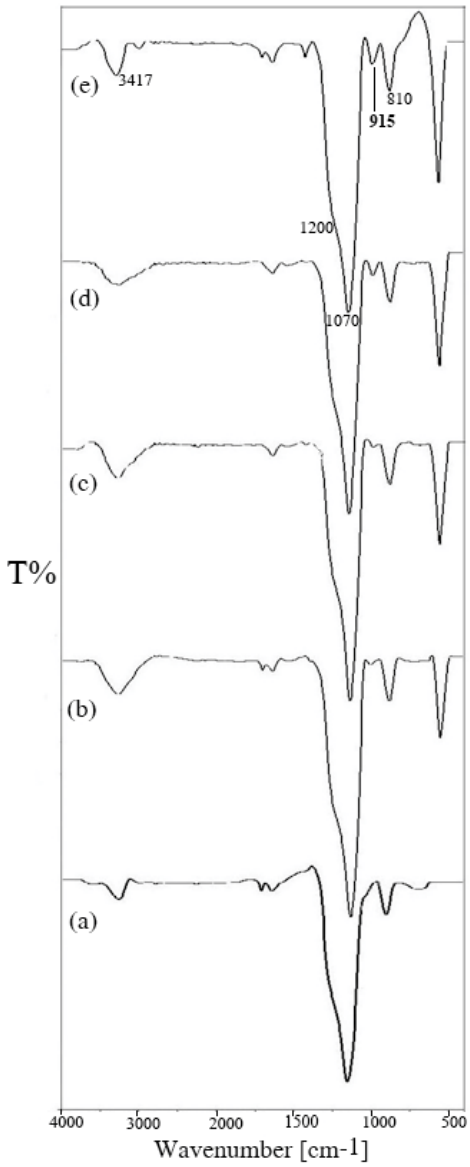

Fig. 1. FTIR spectra of (a)MCF; (b) 1.4V-MCF; (c)2.8V-MCF; (d)4.2V-MCF; (e)5.6V-MCF.

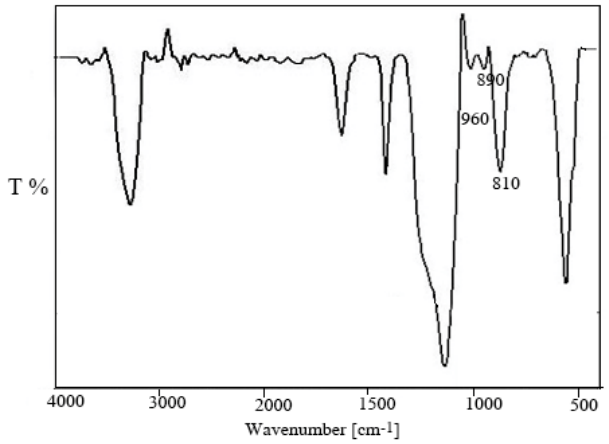

Fig. 2. FTIR spectra of PW_{12}@V-MCF.

The XRD patterns of the PW_{12}@V-MCF samples are illustrated in Fig. 4. It can be observed that the PW_{12} impregnated products are crystalline. But some peaks of PW_{12} overlapped with that of V-MCF. This may be due to the interaction of PW_{12} with that of the support.

3.1.3. BET

The maintenance of the well-defined MCF frameworks after introduction of vanadium or HPA is further supported by the nitrogen sorption data. Fig. 5 shows the N_2 adsorption–desorption isotherms and pore size distributions of MCF silica, V@MCF and PW_{12}@MCF. All the samples exhibited typical IV type isotherms and H1 type hysteresis loops at high relative pressures. This indicated that MCF silica samples with large pore size distribution were successfully prepared. The pore size distribution of the samples shown in the inset of Fig. 5 unambiguously reveals that the 3D mesocellular structure of the support has been preserved.

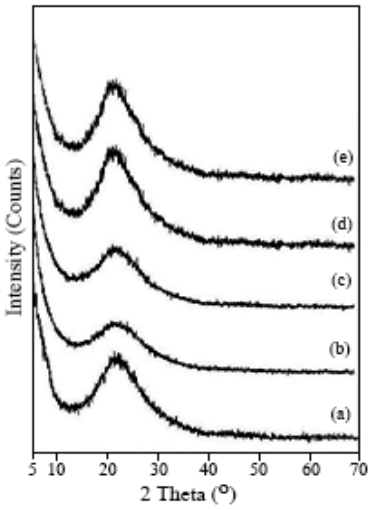

Fig. 3. XRD patterns of (a) MCF; (b)1.4V-MCF; (c) 2.8V-MCF; (d) 4.2V-MCF; (e) 5.6V-MCF.

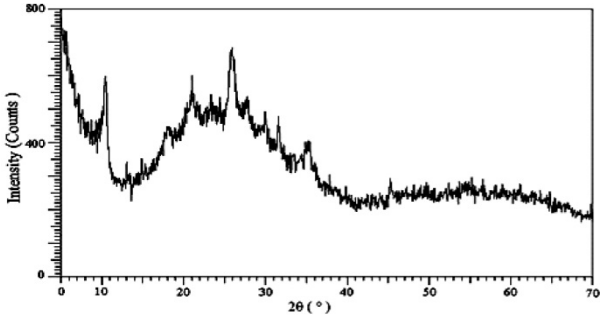

Fig. 4. XRD patterns of PW_{12}@V-MCF.

As expected, the BET surface areas, total pore volumes and mesopore sizes of MCF material are decreased after the functionalization with V or PW_{12} (Table 1). These changes reflect that part of the mesopore volume in the MCF matrix is filled with V or PW_{12}, resulting in pore diameters that are less to that of MCF silica channels.

3.2. Photocatalytic activity

3.2.1. Effect of photocatalyst dosage

The effect of different photocatalytic dosage on the degradation rate of OY has been investigated. The results are shown in Fig 6. It shows the dependence of the OY photodecolorization rate on the catalyst amount. As it indicates, the photodecolorization rate of OY increases with increasing the catalyst and the photodecolorization rate begin to decrease. The photodecomposition rate of the organic pollutant is influenced by the number of the active sites as well as the light absorption ability of the photocatalyst. For a suitable high concentration of the catalyst, the degradation occurs rapidly because more h_{vB+} and e_{CB-} are generated. Excessively high concentration (3 gL^{-1}) of photocatalyst results in decreased photodecolorization rate, which could be attributed to the aggregation of solid particles and shorter light penetration rate brought about by the high absorption coefficient of photcatalyst [43].

In order to calculate photodecolorization rate constant, k values $\ln(C_o/C)$ is plotted as a function of the irradiation time. The rate constant values, k (min^{-1}) are calculated from the slopes of the straight-line portion of the first-order plots as a function of the catalyst mass (Fig. 6 (right)) which are listed in Table 2.

As the results show maximum degradation of OY was observed after 120 min with the maximum rate constant 6.3×10^3 min^{-1} in the presence of 2.5 gL^{-1} of the catalyst for OY.

3.2.2. Effect of initial concentration of the pollutants

The Effect of initial concentration of the OY on the degradation rate was also investigated by varying concentration from 10 mgL^{-1} to 50 mgL^{-1}.

(a)

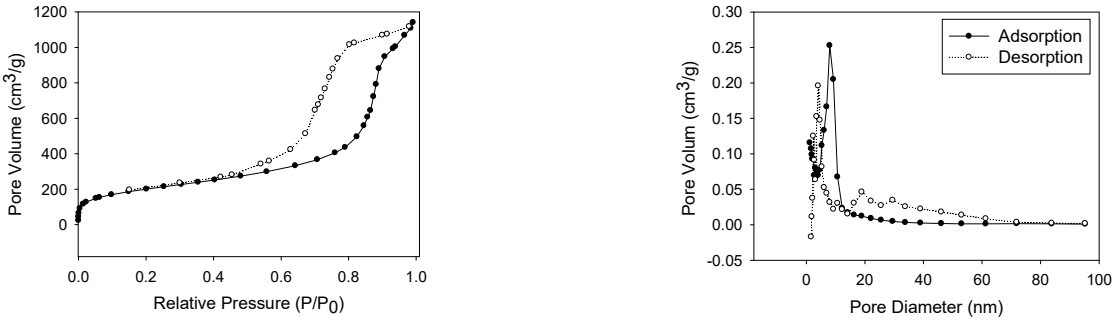

(b)

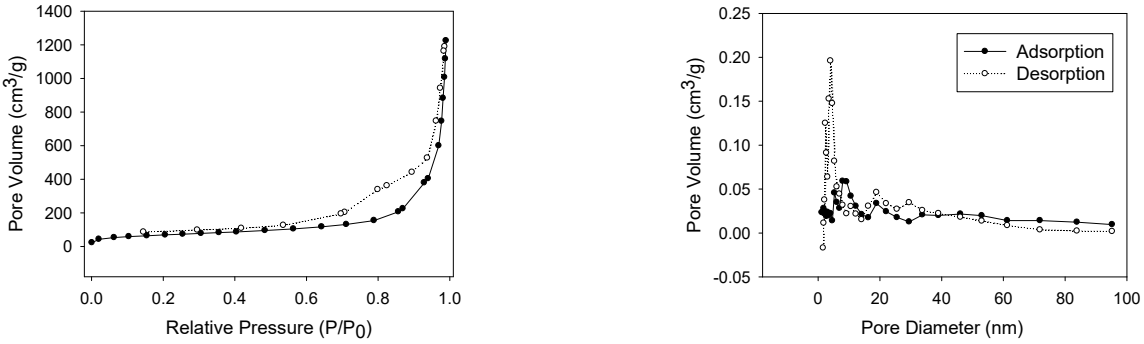

(c)

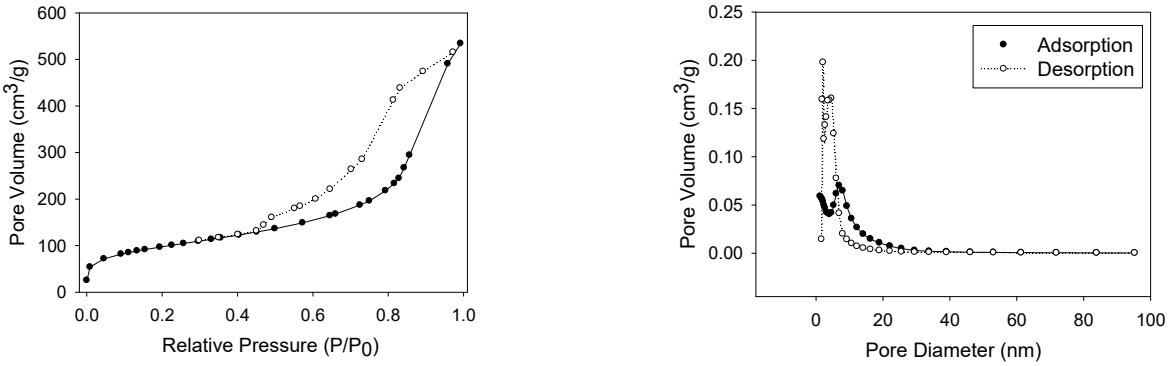

Fig. 5. (Right): N_2-adsorption-desorption isotherms and, (Left): isotherm patterns of pore size distributions of (a) MCF; (b) V-MCF. (c) PW_{12}@V-MCF.

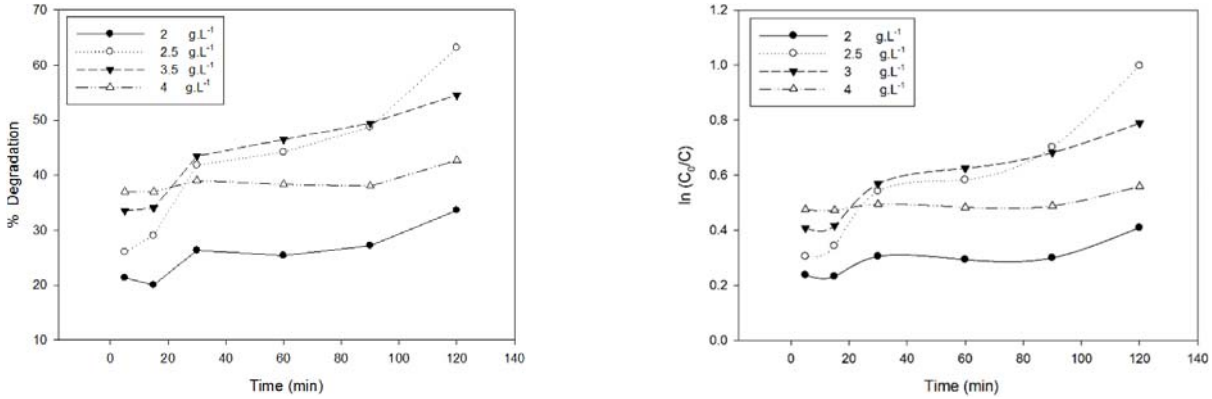

Fig. 6. Effect of dosage of PW_{12}@V-MCF on degradation rate of OY, (initial concentration of OY=25 mg/l and in pH=6.7).

Table 2. Kinetic analysis of the photodecolorization of OY.

Parameter	Value[a]	$k \times 10^3$ (min^{-1})
Catalyst mass (g L^{-1})	0	0
	2	3.1
	2.5	4
	3	3.2
	4	0.6
C_{OY} (mgL^{-1})	10	1.3
	20	4.5
	30	1.8
	40	1.7
	50	1
pH	3	10.3
	5	14.1
	6.8	9.4
	9	4.1
	11	7.1

[a]10 mgL^{-1} OY under dark conditions.

It can be seen from Fig. 7 that the degradation efficiency is decreased with increasing the concentration of OY. The k value are listed in Table 2.

It is obvious that when the concentration is larger than 20 mgL^{-1} the degradation of pollutants will not be effective. This phenomenon can be explained by the following reasons. The first reason is that at higher dye concentration, higher transmission of the solution is reduced to some extent due to UV-screening effect of the dye itself, which in turn causes fewer incident photons to reach the catalyst surface, and it results in a decrease of degradation rate [44].

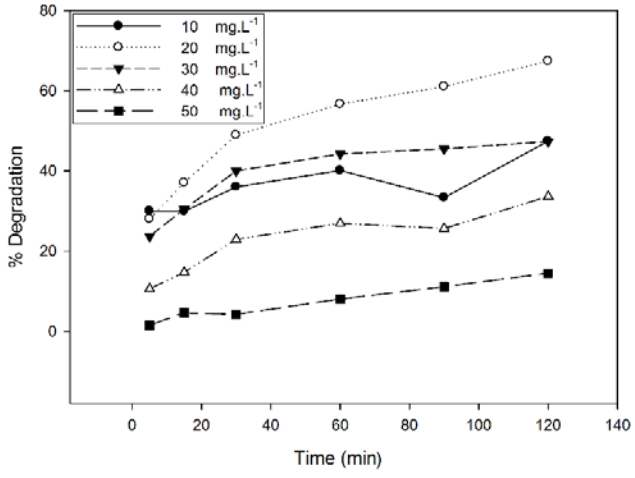

Fig. 7. Effect of initial concentration of the OY on rate of the photodecolorization using 2.5 g L^{-1} of PW_{12}@V-MCF in pH=6.7.

Another reason is that, when the intensity of light source and illumination time are fixed the amount of radicals produced is also a constant [45]. Consequently excess dyes cannot be oxidized and low degradation is obtained at higher OY concentration.

3.2.3. Effect of initial solution pH

One of the important factors in photodecolorization is pH, because the photocatalysis take place on the surface of photocatalyst depends on pH. In order to investigate the effect of pH, the degradation rate and the ph change were measured at different initial pH (Fig. 8).

It is found that the lower pH values of the reaction system and the higher photocatalytic activity of the PW_{12}@V-MCF at pH=1. PW_{12}@V-MCF exhibited the highest photodecolorization efficiency towards OY. Additionally, when pH value is in the range of 2-5, the degradation rate of OY changes a little. However, in the range of pH 6-11, the degradation rate of OY is obviously reduced. Eosin Y is an anionic/acidic dye contains two relatively acidic protons (p*K*a 2.0, 3.8 in water).

The mentioned results suggest that in acidic conditions the surface of the catalyst is positively charged due to the high concentration of H+, so that is favourable to the degradation of OY molecules.

The obviously increased degradation of OY with the decrease of pH value could be interpreted as follows. On the one hand, in acidic condition more H^+ are adsorbed into the photocatalyst and regenerate the catalyst surface sites through timely removal of the intermediate species from the surface [46] thereby improve the degradation of OY. Additionally, it is well known that the absorption of the dye on the catalyst surface directly affects the occurrence of electron transfer between the excited dye and catalyst and it influences the degradation rate.

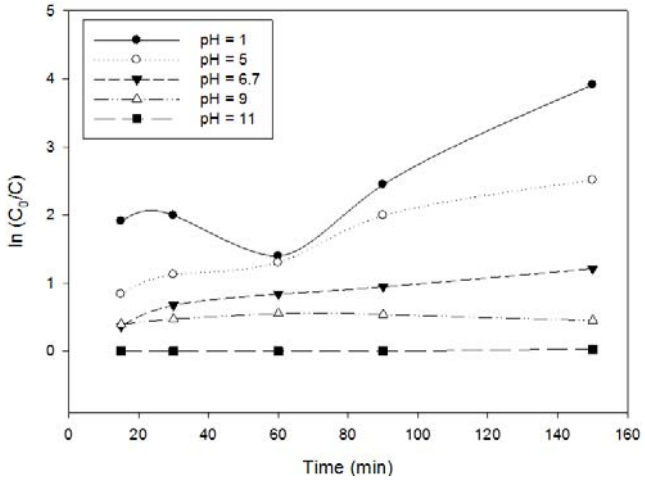

Fig. 8. Effect of solution pH on decolorization efficiency of OY, (initial concentration of the pollutant=20 mg/l and 1 g L^{-1} PW_{12}@V-MCF).

From above discussion, optimum condition for photocatalytic degradation of OY solution (15 ml, C^o= 20 mgL^{-1}) are 2.5 gL^{-1} dose of catalyst and pH=1. Fig. 9 shows the photocatalytic behaviour of PW_{12}@V-MCF under optimum conditions. The PW_{12}@V-MCF catalyst can be easily separated and recovered and the deactivation of the catalysts was observed after four catalytic activity (Table 2).

As shown in Fig. 9, monitored UV-vis spectra of OY using PW_{12}@V-MCF as the photocatalyst indicate that UV-vis intensities of OY decrease obviously upon irradiation that confirm the photocatalytic activity property of PW_{12}@V-MCF.

In order to determine the degradation of substrates, photolysed solution (300 $mg.L^{-1}$) of the OY were analysed by HPLC. The HPLC chromatograms show the degradation of pollutant into smaller fragments, which are subsequently mineralized completely. A sharp peak of the dye was detected at 0 h irradiation; whereas, only 11.8% was observed at the end of 2h. The dye peak showed a significant decrease at the end of 2h and some new peaks were observed at different retention times during irradiation which confirmed the formation of degradation products.

3.2.4. Reusability

Apart from presenting a good catalytic activity, long-term stability and the absence of leaching are of primary importance for solid catalysts. In order to determine if the photocatalyst suffered from permanent deactivation, PW_{12}@V-MCF was reused several times. The standard procedure, described in the experimental section, was followed to perform the 1st-3rd runs. The wet catalyst was recycled and no appreciable change in activity was noticed after three cycles (Table 3).

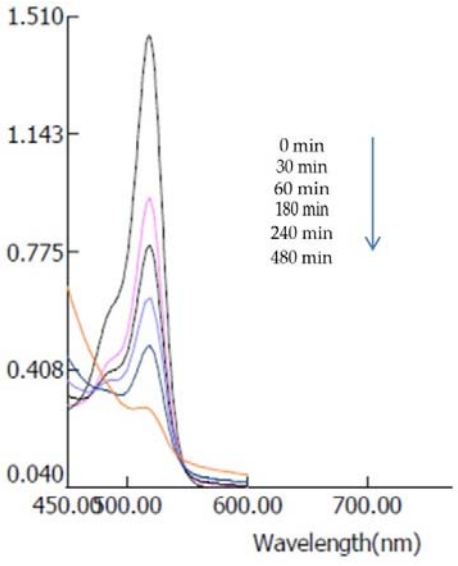

Fig. 9. Changes in the UV-vis absorption specta of OY in o optimized conditions.

After the third run, the PW_{12} were leached from the supports (shown by NAA), and this led to the deactivation of the heterogeneous catalyst. It is well known that due to solubility of PW_{12} in polar solvents, PW_{12} leaching will be significant from PW_{12}@support system.

4. Conclusions

$H_3PW_{12}O_{40}$ impregnated on V-MCF is very active as a photocatalyst towards photodecolorization of OY. Undoubtedly the MCF matrix provides a better dispersion of active sites and free accesses of the dyes molecules to these isolated sites, thereby facilitating in photocatalytic activity. The present study however, my serve as a preliminary step towards designing further studies on the photochemical aspect being in our laboratory at present.

High specifies surface area of PW_{12}@V-MCF would result in high catalytic activity because the active sites (W-O-W bonds) were better spread on the surface and in the micropores of silica matrix.

Acknowledgements

We gratefully thank Shahreza Branch, Islamic Azad University, for financial support.

References

[1] C. Galindo, P. Jacques, A. Dalt, Chemosphere 45 (2001) 997-1005.
[2] J.M. Herrmann, M. Vautier, C. Guillard, J. Catal. 201 (2001) 46-59.
[3] U. Pagga, K. Taeger. Water Res. 28 (1994)1051-1057.
[4] M.R. Hoffmann, S.T. Martin, W. Choi, D.W. Bahnemann. Chem. Rev. 95 (1995) 69-96.
[5] B. Neppolian, S. Sakthivel, M. Palanichamy, B. Arabindoo, V. Murugasen, Stud. Surf. Sci. Catal. 113 (1998) 329-335.
[6] J. Guo, Y. Li, S. Zhu, Z. Chen, Q. Liu, D. Zhang, W.J. Moon, D.M. Song, RSC Adv. 2 (2012) 1356-1363.
[7] R. Dillert, D. Bahnemann, H. Hidaka, Chemosphere 67 (2007) 785-792.
[8] M.H. Habibi, E. Askari, Iran. J. Catal. 1 (2011) 41-44.

Table 3. Investigation of the feasibility of reusing of PW_{12}@V-MCF in the photodegredation of OY.

Run	Degradation (%)	Amount of W leached (%)[a]
1	98	-
2	96	-
3	93	-
4	43	0.07

[a]Determined by NAA.

[9] H. Faghihian, A. Bahranifard, Iran. J. Catal. 1 (2011) 45-50.
[10] A. Nezamzadeh-Ejhieh, M. Khorsandi, Iran. J. Catal. 1 (2011) 99-104.
[11] H. R. Pouretedal, S. Basati, Iran. J. Catal. 2 (2012) 51-55.
[12] A. Nezamzadeh-Ejhieh, Z. Banan, Iran. J. Catal. 2 (2012) 79-83.
[13] A. Bagheri Ghomi, V. Ashayeri, Iran. J. Catal. 2 (2012) 135-140.
[14] H. R. Pouretedal, M. Ahmadi, Iran. J. Catal. 3 (2013) 149-155.
[15] K.Y. Ho, G. McKay, K.L. Yeung, Langmuir 19 (2003) 3019–3024.
[16] R.K. Dey, F.J.V.E. Oliveira, C. Airoldi, Colloid Surf. A 324 (2008) 41–46.
[17] X. Feng, G.E. Fryxell, L.O. Wang, A.Y. Kim, J. Liu, K.M. Kemner, Science 276 (1997) 923–926.
[18] M.H. Lim, A. Stein, Chem. Mater. 11 (1999) 3285–3295.
[19] A. Pearson, S. K. Bhargava, V. Bansal, Langmuir 27 (2011) 9245-9252.
[20] C. Yang, Y. Changjun, L. Tian, L. Ye, T. Peng, K. Deng, L. Zan, J. Appl. Polymer Sci. 120 (2011) 2048-2053.
[21] Z. Jiang, J. Han, X. Liu, Adv. Mater. Res. 152-153 (2011) 202-207.
[22] Y.W. Chang, N.J. Kim, C.S. Lee, Adv. Mater. Proc. 26-28 (2007) 1083-1987.
[23] C. Chen, Q. Wang, P. Lei, W. Song, W. Ma, J. Zhao, Environ. Sci. Tech. 40 (2006) 3965-3970.
[24] K. Lv, Y. Xu, J. Phys. Chem. B 110 (2006) 6204-6212.
[25] H. Einaga, M. Misono, Bull. Chem. Soc. Jpn. 69 (1996) 3435-3441.
[26] A. Mylonas, A. Hiskia, E. Papaconstantinou, J. Mol. Catal. A: Chem. 114 (1996191-200.
[27] A. Molinari, R. Amadelli, V. Carassiti, A. Maldotti, Eur. J. Inorg. Chem. (2000) 91-96.
[28] D.A. Friesen, L. Morello, J.V. Heaaley, C.H. Langford, J. Photochem. Photobio. A: Chem. 133 (2000) 213-220.
[29] R.D. Gall, C.L. Hill, J.E. Walker, Chem. Mater. 8 (1996) 2523-2529.
[30] N. Mizuno, M. Misono, Chem. Rev. 98 (1998) 199-217.
[31] L.K. Kolkova, E.S. Rudakov, V.P. Tretyakov, Kinet. Katal. 37 (1996) 540-554.
[32] Y. Guo, Y. Wang, C. Hu, E. Wang, Chem. Mater. 12 (2000) 3501-3508.
[33] Y. Guo, D. Li, C. Hu, Y. Wang, E. Wang, Y. Zhou, S. Feng, Appl. Catal. B 30 (2001) 337-349.
[34] A. Nezamzadeh- Ejhieh, S. Hushmandrad, Appl. Catal. A 388 (2010) 149-159.
[35] H. Salavati, N.Tavakkoli, M. Hosseinpoor, Ultrason. Sonochem. 19 (2012) 546–553.
[36] L. You-ji, C. Wei, Catal. Sci. Technol. 1 (2011) 802–809.
[37] J.S. Lettow, Y.J. Han, P. Schmidt-Winkel, P. Yang, D. Zhao, G.D. Stucky, J.Y. Ying, Langmuir 16 (2000) 8291-8295.
[38] F. Gao, Y. Zhang, H. Wan, Y. Kong, X. Wu, L. Dong, B. Li, Yi Chen, Microporous Mesoporous Mater. 110 (2008) 508-516.
[39] F. Cavani, N. Ballarini, A. Cericola, Catal. Today 127 (2007) 113-131.
[40] F. Ying, J. Li, C. Huang, W. Weng, H. Wan, Catal. Lett. 115 (2007) 137-142.
[41] M. Piumetti, B. Bonelli, M. Armandi, L. Gaberova, S. Casale, P. Massiani, E. Gar- rone, Microporous Mesoporous Mater. 133 (2010) 36-44.
[42] M. Piumetti, B. Bonelli, P. Massiani, Y. Millot, S. Dzwigaj, M. Armandi, L. Gaberova, E. Garrone, Microporous Mesoporous Mater. 142 (2011) 45-54.
[43] M.A. Barakat, H. Schaeffer, G. Hayes, S. Ismat-Shah, Appl. Catal. B 57 (2005) 23–30.
[44] Y. Zhang, J. Wan, Y. Ke, J. Hazard. Mater. 177 (2010) 750–754.
[45] D. Priya, J. Modak, A. Raichur, ACS Appl. Mater. Interfaces 1 (2009) 2684–2693.
[46] Q. Wang, M. Zhang, C. Chen, W. Ma, J. Zhao, Angew. Chem. Int. Ed. 49 (2010) 7976–7979.